DOI: 10.1002/adma.200502026

Self-Assembly Process to Integrate and Connect Semiconductor Dies on Surfaces with Single-Angular Orientation and Contact-Pad Registration**

By *Wei Zheng* and *Heiko O. Jacobs**

The construction of man-made artifacts such as cell phones and computers relies on robotic assembly lines that place, package, and interconnect a variety of devices that have macroscopic (> 1 mm) dimensions.[1] The key to the realization of these systems is our ability to integrate/assemble components in 2D/3D as well as link/interconnect the components to transport materials, energy, and information. The majority of these systems that are on the market today are heterogeneous in nature. Heterogeneous systems can be characterized as systems that contain at least two separate parts that prohibit monolithic integration. Such systems are typically fabricated using robotic pick and place. The size of the existing systems could be reduced by orders of magnitudes if microscopic building blocks could be assembled and interconnected effectively.[2] The difficulty is not the fabrication of smaller parts but the assembly and formation of interconnects. For components with dimensions less than 100 μm, adhesive capillary forces often dominate gravitational forces, making it difficult to release the components from a robotic manipulator.[3] Micromanipulator-based assembly and wafer-to-wafer transfer methods work poorly on non-planar surfaces, in cavities, and in the fabrication of 3D systems. Serial processes, in general, are slow. Conventional robotic methods and assembly lines are challenged because of the difficulty in building machines that can economically manipulate parts in three dimensions that are only micrometers in size.[4]

At another extreme, nature forms materials, structures, and living systems by self-assembly on a molecular length scale.[5,6] As a result, self-assembly-based fabrication strategies are widely recognized as inevitable tools in nanotechnology and an increasing number of studies are being carried out to "scale up" these concepts to close the assembly gap between nanoscopic and macroscopic systems. Recent demonstrations of processes that can assemble micrometer- to millimeter-sized components include: shape-directed fluidic methods that position electronic devices on planar surfaces using shape recognition and gravitational forces,[7,8] liquid-solder-based self-assemblies that use the surface tension between pairs of molten solder drops to assemble functional systems,[9–11] capillary-force-directed self-assembly that uses hydrophilic/hydrophobic surface patterns and photocurable polymers to integrate micro-optical components, micromirrors, and semiconductor chips on silicon substrates,[12–14] and shape-and-solder-directed self-assembly that combines geometrical shape recognition with site-specific binding involving liquid solder to assemble and package heterogeneous microsystems. [15–17] While all of these methods share the common feature of providing parallel assembly on a large scale, process parameters and design rules remain not well characterized. Another great challenge is the realization of heterogeneous systems that contain many different parts and enable contact-pad registration.[16] While current methods allow the positioning of a large number of identical components in a massive parallel manner, systems that consist of more than one repeating unit are difficult to build. Recent studies to overcome this problem include the activation of selected receptors to enable batch transfer on desired locations,[18–20] and a sequential self-assembly process that uses geometrical shape recognition for component registration and surface tension, involving liquid solder to form mechanical and electrical connections.[15–17] In both cases, batches of components are added sequentially to build the system, as opposed to adding all components at the same time.

In this communication we present a study on controlling angular orientation and contact-pad registration during the self-assembly process. The presented process can be seen as an extension of prior work[9–11,15–17] in the area of surface-tension-directed self-assembly involving liquid solder to form interconnects and is compatible with these processes. Angular-orientation control is important because dies, packaging, or optical elements need to be placed on a substrate with correct angular orientation to enable contact-pad registration or device operation. Angular-orientation control has been challenging in self-assembly. For example, Srinivasan et al. assembled silicon components and micromirrors onto a gold-coated silicon substrate using hydrophilic/hydrophobic interactions and a non-conducting adhesive lubrication layer. The assembly of 98 parts, 500 μm in size, was accomplished with 0.3° rotational precision.[12] However, due to the square-shaped binding and receptor sites four stable angular orientations, 0, 90, 180, and 270°, were observed. While Liang et al.

[*] Prof. H. O. Jacobs, Dr. W. Zheng
Department of Electrical and Computer Engineering
University of Minnesota
200 Union Street SE, Minneapolis, MN 55455 (USA)
E-mail: hjacobs@ece.umn.edu

[**] This work was supported by the National Science Foundation (grant ECS-0300263 and ECS-0601454.

ADVANCED MATERIALS

optimized the designs of the receptors and binding sites to remove local energy minima and achieve unique orientation and alignment,[21] unique offset ring patterns with specific geometric constraints are required for their method. Most recently, studies have focused on the use of gravitational forces with components that have a peg and a hole on a substrate on a tilted surface to accomplish assembly with single-angular orientation.[22] The formation of electrical interconnects and contact-pad registration has not been possible using the surveyed methods. The key building blocks of the presented self-assembly process that enables the assembly of standard die forms with single-angular orientation and contact-pad registration are "two-element docking sites" on the substrate that contain alignment pedestals (out of silicon or photoresist) and solder-coated areas commonly used in printed circuit boards. These two elements—alignment pedestals and solder-coated areas—are designed according to the size and shape of the components, in particular the location and shape of the contact pads. The angular-alignment capability is gained as a result of the combination of these two elements. During the self-assembly process the agitated components attach to the solder-coated areas only after a correct angular preorientation condition is met; differently sized components can be integrated using sequential batch transfer on substrates presenting different docking-site layouts. Assembly of multisized components without electrical interconnects has been demonstrated previously using a process that required precise complementary shape recognition.[23,24] Conceptually, this work is different in the sense that the process integrates components on a surface and in the sense that the docking site acts as a chaperone to guide the assembly process, preventing defects; precise complementary shapes are no longer required and would slow down the assembly process. The technological focus of the presented work is the assembly of commonly used die forms, most of which are square in shape and cannot be integrated with single-angular orientation using existing methods while supporting the formation of electrical interconnects. The components that we tested in this study were standard silicon dies and glass components. Arrays containing one hundred identical components as well as a mix of two components (900 and 500 μm in size) were prepared using the procedure. First, design rules were identified to accomplish self-assembly with an angular-orientation accuracy of 0.3° and filling factors of 100 %.

The experimental strategy to assemble and connect components on surfaces with single-angular orientation and contact-pad registration is illustrated in Figure 1. The components were integrated on a substrate using solder-coated areas that were partially surrounded with raised u-shaped alignment pedestals. The components can only attach to the solder-coated areas if a correct angular preorientation condition is met: components that arrive at the docking sites with an angular orientation that deviates by more than ±90° from the desired orientation will not find a sufficient overlap between the binding site (contact area) on the components and the solder-coated areas on the substrate and will not attach; other components will be captured and aligned due to the reduction of the interfacial free energy.

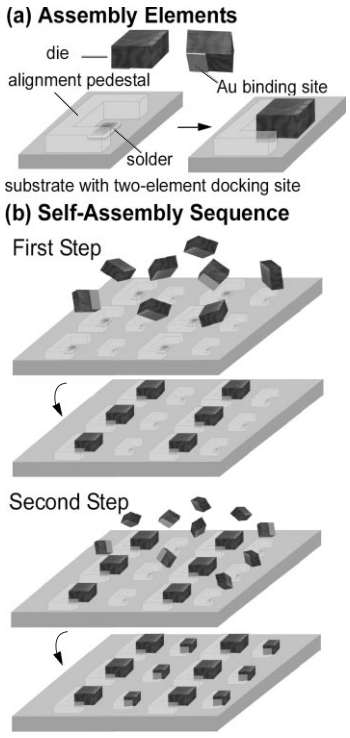

Figure 1. Strategy to assemble and connect chip-scale components with different dimensions, single-angular orientation, and contact-pad registration. a) Self-assembly elements depicting dies with a gold contact and two-element docking sites containing alignment pedestals and solder-coated areas. b) Two-step self-assembly sequence to populate the substrate with different components. The reduction of the interfacial free energy drives the assembly process into a stable position.

As a first demonstration, we focused on silicon dies that carried rectangular gold-coated areas on the back, and square-shaped contacts and alignment marks on the front. The outlined procedure shows the sequential batch assembly for silicon components with different dimensions. We tested the sequential batch assembly of (900 × 900 × 500) μm silicon dies in the first self-assembly step and (500 × 500 × 500) μm in the second step. Aside from the depicted components that carry a single contact on the back we tested the directed-assembly strategy using glass components that carried seven contacts on one face and the assembly of these components at designated areas on a surface using a "flip-chip" orientation. The procedures used to fabricate the silicon, glass components, pedestals, and solder-coated areas are described in the Experimental section. During the self-assembly the surface of the liquid solder wets and binds to the gold-coated contact on the back side of the dies. Energy minimization drives the assembly into a stable single-angular orientation. The solder also provides the mechanical bond required to hold the assembly together. We used, both, low- (47 °C) and medium- (138 °C) melting-point (mp) solders (Y-LMA-117 and LMA-281, Small Parts, Miami Lakes, FL) that were used in previous self-as-

sembly experiments;[11,17,25] we did not observe a notable difference between the two. The assembly was performed in a glass beaker (100 mm in diameter) that was filled with ethylene glycol at a temperature of 150 °C, at which temperature the solder was molten. Ethylene glycol was used to accommodate the higher-mp solder that is not compatible with a water-based assembly solution and because it prevents the formation of trapped air bubbles in recessed areas. The ethylene glycol solution was made slightly acidic (pH ~ 2.5) with sulfuric acid to remove metal oxide from the surface of the solder drop; an oxide layer—if sufficiently thick—blocked the wetting of the metal surface. Component transport and mixing was provided by hand using a constant horizontal orbital motion while tilting the beaker up and down so that the components tumbled randomly across the surface; the component transport method needs to be automated in future work using a fluidic conveyor-belt-type system.

Figure 2 shows the result of batch-assembled silicon components with single-angular orientation and contact-pad registration using both the silicon (Fig. 2a,b) and SU-8 alignment pedestals (Fig. 2c,d). The first result (Fig. 2a,b) shows a two-component 10 × 10 array that contains 900 μm and 500 μm dies that were assembled using the two-step self-assembly sequence, while the lower half (Fig. 2c,d) shows a single-component 10 × 10 array that was used to determine the alignment accuracy. The alignment was measured for the entire array using a set of top-view scanning electron microscopy (SEM) images—Figure 2d shows a representative example—that were overlaid with a grid of squares that had a constant pitch and angular orientation. The required displacement and rotation of the overlaid squares to match the actual assembly was measured using AutoCAD 2000 software (Autodesk, San Rafael, CA). The results are depicted in Figure 2e. We found a systematic error of 0.8° in the angular orientation that resulted from an angular-misalignment error that was made by the operator during the dicing of the dies. The shift towards positive values is visible in the histogram for the angular orientation. The accuracy of the self-assembly process was determined using the standard deviation which was 0.3° for the angular orientation and 19 μm for lateral accuracy. The recorded values were limited by the accuracy of the dicing saw (grit size 15 μm, Disco DAD 2H/6T, Disco, Santa Clara, CA) and may improve if higher-precision components are used. We carried out these self-assembly experiments a number of times and found that it is necessary to use excess dies in the assembly suspension. Without excess dies we were not able to completely populate the substrate using the random motion. Excess dies were recycled between experiments. The illustrated results were accomplished using an assembly suspension that contained 500 dies. Complete coverage of the respective receptors was accomplished in 5 min for Figure 2a and b and 3 min for Figure 2c and d. All experiments were repeated three times; we obtained complete coverage each time.

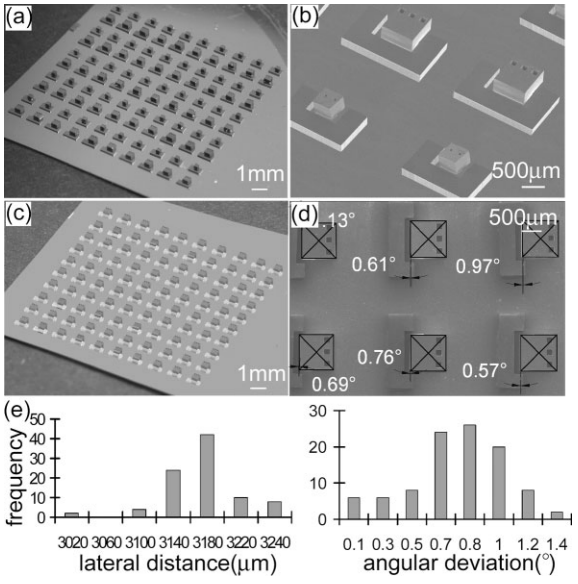

Figure 2. Photographs and SEM images of silicon dies that have been assembled using a combination of alignment pedestals, solder-coated areas, and sequential batch transfer. a) Photograph and b) SEM image of a 10 × 10 array that contains alternating rows of 900 μm and 500 μm dies that are surrounded by Si alignment pedestals. c) Photograph of a 10 × 10 array with SU-8 alignment pedestals that was used to study the alignment accuracy. d) Representative SEM close-up and overlay that illustrates how the center-to-center distance and angular-orientation accuracy was determined. e) Histograms of the measured values.

During the course of this study we observed that the width, length, and height of the alignment pedestals were important parameters that affected the assembly process and yield. At first, we started the experiment without alignment pedestals. Figure 3a shows a number of conformations that were observed. Without alignment pedestals four angular orientations 0°, 90°, 180°, and 270° were apparent, which were evenly populated for square-shaped receptor/binding sites, while two orientations were favored for rectangular designs. The two-fold symmetry was sufficiently disturbed for a 2:1 side-to-length ratio which favors 0° and 180° angular orientation (Fig. 3a, a1 and a2). The 90° and 270° angular-orientation results were not recorded experimentally unless two components assembled onto a single receptor at the same time, which occurred in less than 2 % of the cases (Fig. 3a, a3). The results without alignment pedestals were consistent with other asymmetric binding site/receptor designs (triangles, L shapes, spiral-type drops)[14] that generally favor one orientation but fail to completely remove defects due to local energy minima in the space of possible conformations. To design self-assembly systems with alignment pedestals, we started with computer-aided designs (CADs) of the components and different designs of alignment pedestals. The components were rendered semitransparent and arranged in the CAD tool to find different conformations that had an overlap with the binding site while modifying the design of the alignment pedestals to remove defects. This CAD procedure allows for the optimization of the geometrical parameters including alignment-pedestal design and component design by placing the components at different angles

ADVANCED MATERIALS

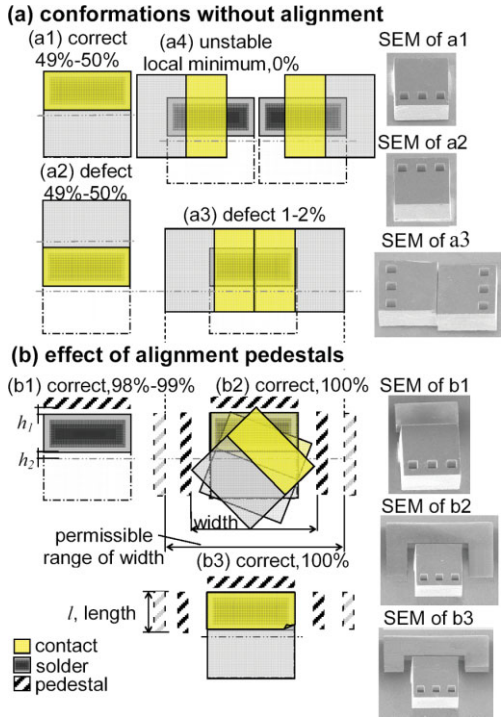

Figure 3. Semitransparent component arrangements that illustrate the computer-aided design (CAD) design approach that is used to eliminate defects and establish design rules together with experimental results. a) Rectangular receptor/binding site design that favors the 0° and 180° (a1 and a2) angular orientation along with predictions of defects (a3) and (a4). The predicted defect where two components assemble on a single receptor (a3) was recorded experimentally in 1–2 % of the cases. The 90° and 270° orientation with a single component (a4) was not observed. b) Alignment-pedestal designs to eliminate defects. b1) Single-pedestal designs with $h_1 \leq h_2$ eliminate the 180° conformational overlap and yield the correct orientation in 98 % of the cases. b2,b3) Pedestals on the side eliminate the attachment of two components. l and w indicate the permissible range of the opening to ensure defect-free assembly.

on the surface to study possible conformations and defects. Through a number of iterations we obtained design rules that supported assembly without defects. Figure 3b illustrates this design approach alongside experimental results. Introducing the alignment pedestals was effective in removing the defects illustrated in Figure 3a. To remove incorrect orientations, we started with one pedestal along the elongated side (b1), performed the assembly experiment three times and found that this design accomplished correct angular orientation in 98 % of the cases if certain design rules were considered. For example, the clearance h_1 between the solder and alignment pedestal needs to be equal or smaller than the distance h_2 between the binding site (metal contact) and center line on the component to prevent partial overlap for the 180° angular orientation. We used $h_1 = h_2 = 50$ μm in our design to leave some clearance for the components to adjust their position. Furthermore, the binding site needs to be sufficiently large to ensure that the components adhere to the substrate during the self-assembly process. As a first-order approximation, the capillary energy gain and energy of adhesion was proportional to the overlap between the receptor on the substrate and the metal-coated binding site on the component.[14] In the illustrated designs, the solder-coated areas on the substrate and the binding sites on the components had the same dimensions to provide maximum overlap. Experimentally, we observed that the adhesion was sufficiently strong if the metal binding sites occupied at least 30 % of the footprint of the component; below this limit components detached during the self-assembly.

In order to remove the remaining 2 % defects where two components assembled next to each other, we added alignment pedestals on the side of the solder-coated area (b2). The opening w needs to be smaller than twice the component size and larger than the diagonal length of the components, such that the components can rotate freely. Within this permissible range larger widths allowed a slightly fast assembly rate. We performed a number of assembly experiments using this design that yielded defect-free assemblies in all cases.

In the last design we changed the length (l) of the pedestal opening (b3) and noticed that this parameter was not critical in terms of yield; however, it did influence the assembly speed. The time to complete the defect-free assembly was reduced from 4–5 min for design b2 to 3 min for design b3. A representative image using design b3 is shown in Figure 2d. Design b1, without alignment pedestals on the sides, had the fastest assembly rate—it took 2 min to reach completion.

The assembly process follows similar design rules to assemble the different-sized components that were illustrated in Figure 2a and b. The additional consideration is that the opening should be designed to avoid 900 μm components assembling into the docking sites that were designed for 500 μm components. We used design b2 with two 800 μm and 1.4 mm openings in this case. The design strategy can be extended to the flip-chip assembly of components and dies that carry more than one contact. An initial result is illustrated in Figure 4 that used glass components that were made from borofloat glass wafers (Universitywafer, Boston, MA). Each component had seven gold contact pads, two on the left, and five on the right. The five contacts on the right were coated with a high-mp solder (Y-LMA-281, mp ~138 °C, Small Parts, Miami Lakes, FL) and protected with photoresist to prevent misorientation during the self-assembly. Each docking site contained two corresponding gold contacts carrying a low-mp

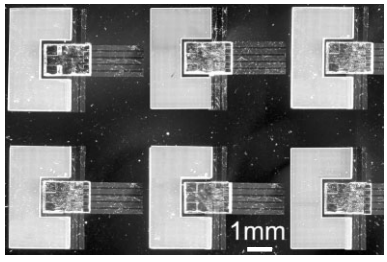

Figure 4. Glass components with multicontacts assembled into a substrate by single-angular orientation self-assembly.

solder (Y-LMA-117, mp ~47 °C Small Parts, Miami Lakes, FL) on the left and five gold contacts on the right connecting with the gold wires on the substrate. The low-mp solder is used to drive the assembly and ensure correct angular orientation during the self-assembly. The assembly was performed in ethylene glycol at a temperature of 100 °C instead of 150 °C that was used for the earlier experiments described above. After completion of the self-assembly the entire structure was heated to 150 °C to establish the seven contacts. Electrical connectivity with a contact resistance of less than 2 Ω was confirmed in all cases. Alternatively, the high-mp solder could be integrated on the substrate instead of components.

We have demonstrated the directed self-assembly of micrometer-sized components with single-angular orientation accuracy of 0.3° and contact-pad registration with an accuracy of 19 μm for 500 μm–2 mm components. While the feasibility has been tested we have not yet established the ultimate complexity in terms of alignment accuracy, number of contacts, and density of interconnects that could be established by this process. First, design rules have been established to enable batch transfer of differently sized components onto surfaces without defects. The graphical CADs of the shapes and binding sites were found to be very efficient in predicting the outcome of the self-assembly as well as in identifying and eliminating potential defects. We believe that combinatorial methods that combine geometrical shape recognition, surface tension, sequential self-assembly, and programmable self-assembly that activates receptors[15,17,20] are necessary to achieve the required flexibility in the design of heterogeneous systems on both the micro- and nanometer length scale with minimal defects.

Experimental

All the components were fabricated using standard photolithography and surface micromachining. As photomasks we used a rapid prototyping approach that uses a high-resolution laser printer (Linotype Herkules Imagesetter, Heidelberg, Germany) to create 5080 dpi prints onto transparency films instead of commonly used chrome masks that take some time to fabricate. The transparency films were mounted onto a glass plate that fits into the mask aligner. The minimum feature size using the transparency films was ca. 40 μm and line roughness was ca. 10 μm.

Fabrication of the Silicon and Glass Components: In brief, the silicon blocks and glass components were made using standard photolithography and surface micromachining from p-type silicon wafers and borofloat glass wafers (Universitywafer, Boston, MA), respectively. Alignment marks on the top were formed by spin-coating Shipley 1075 photoresist (Shipley, Phoenix, AZ) at 3000 rpm onto the wafer, UV exposure through a shadow mask for 80 s, development in MIF-351 1:5 developer for 2 min, and etching in a deep-trench etcher (SLR-770, Plasmatherm, North St. Petersburg, FL) for 1 h. The contact pad on the back was formed by coating 25 nm of chrome and 500 nm of gold using an electron-beam evaporator. Shipley 1813 photoresist (Shipley, Phoenix, AZ) was spin-coated at 4000 rpm, exposed through a shadow mask for 7 s, and developed in MIF-351 1:5 developer for 15 s to expose the underlying metal areas that were subsequently removed by etching using 4 KI:1 I_2:40 H_2O for gold and 1 HCl:1 Glycerol:3 H_2O for chrome. Finally, we diced the wafers using a fully automated dicing saw to obtain the components. The glass components did carry contact pads on a single side and no alignment marks on the front. The contact pads were made of gold and five of them were protected with Shipley 1813 photoresist. The protection was necessary to ensure correct angular orientation.

Fabrication of the Silicon and SU-8 Pedestals and Solder-Coated Areas: The pedestals were fabricated, either by deep-trench etching silicon or using SU-8 photoresist. The etched silicon pedestals were formed by spin-coating Shipley 1075 photoresist (Shipley, Phoenix, AZ) at 3000 rpm onto a 500 μm thick p-silicon wafer, followed by UV exposure through a shadow mask for 80 s, development in MIF-351 1:5 developer for 2 min, and etching in a deep-trench etcher (SLR-770, Plasmatherm, North St. Petersburg, FL) for 3 h. The patterned protective photoresist was removed in acetone to expose the 300 μm tall silicon pedestals underneath.

The pedestals out of SU-8 were formed by spin-coating Nano SU-8 2001 photoresist (Microchem, Newton, MA) at 1000 rpm onto a 500 μm thick p-silicon wafer, followed by a two-step soft bake at 65 °C for 7 min and 95 °C for 60 min on a hotplate, UV exposure through a shadow mask for 60 s, post-exposure bake at 65 °C for 1 min and 95 °C for 15 min on a hotplate, and development in PM acetate developer for 60 min.

Following the fabrication of pedestals, the wafers were started by coating 25 nm titanium and 500 nm copper using an electron-beam evaporator. Shipley 1805 photoresist (Shipley, Phoenix, Arizona) was spin-coated at 1000 rpm, exposed through a shadow mask for 30 s, and developed in MIF-351 1:5 developer for 60 s to expose the underlying metal areas that were subsequently removed by etching using a ferric chloride solution (1.4 g of $FeCl_3$ per milliliter of H_2O, pH 1.3, 20 s) for copper and 40 % NH_4F/49 % HF 10:1 buffered oxide etchant for titanium for 15 s. The remaining copper squares were coated with solder by removing the protective photoresist in acetone and by immersing the wafer into a solder bath until each copper square was coated with solder. The solder bath carried a layer of water on top that contained small amounts of sulfuric acid (pH 2) which is necessary to maintain an oxide-free solder surface. Immersing the wafers through the acidic water also helped remove any oxide on the copper surface that might have formed during the process before it was brought into contact with the solder. A clean copper surface was necessary for the wetting to take place.

Received: September 22, 2005
Final version: February 9, 2006
Published online: April 26, 2006

[1] M. B. Cohn, K. F. Bohringer, J. M. Noworolski, A. Singh, C. G. Keller, K. Y. Goldberg, R. T. Howe, *Proc. SPIE-Int. Soc. Opt. Eng.* **1998**, *3512*, 2.
[2] T. D. Clark, J. Tien, D. C. Duffy, K. E. Paul, G. M. Whitesides, *J. Am. Chem. Soc.* **2001**, *123*, 7677.
[3] R. S. Fearing, presented at the *IEEE/RSJ Int. Conf. on Intelligent Robots and Systems*, Pittsburgh, PA, USA, August 1995.
[4] M. Walz, *Circuits Assembly* **2003**, *1*, 32.
[5] S. Zhang, *Nat. Biotechnol.* **2003**, *21*, 1171.
[6] G. M. Whitesides, B. Grzybowski, *Science* **2002**, *295*, 2418.
[7] H. J. J. Yeh, J. S. Smith, *IEEE Photon. Technol. Lett.* **1994**, *6*, 706.
[8] J. S. Smith, H. J. J. Yeh, *US Patent 5 824 186*, **1998**.
[9] D. H. Gracias, J. Tien, T. L. Breen, C. Hsu, E. M. Whitesides, *Science* **2000**, *289*, 1170.
[10] M. Boncheva, D. H. Gracias, H. O. Jacobs, G. M. Whitesides, *Proc. Natl. Acad. Sci. USA* **2002**, *99*, 4937.
[11] H. O. Jacobs, A. R. Tao, A. Schwartz, D. H. Gracias, G. M. Whitesides, *Science* **2002**, *296*, 323.
[12] U. Srinivasan, D. Liepmann, R. T. Howe, *J. Microelectromech. Syst.* **2001**, *10*, 17.
[13] U. Srinivasan, M. A. Helmbrecht, C. Rembe, R. S. Muller, R. T. Howe, *IEEE J. Select. Topics Quantum Electron.* **2002**, *8*, 4.

[14] K. F. Boringer, U. Srinivasan, R. T. Howe, presented at the *IEEE Int. Conf. on Micro Electro Mechanical Systems (MEMS)*, Interlaken, Switzerland, January **2001**.
[15] W. Zheng, P. Buhlmann, H. O. Jacobs, *Proc. Natl. Acad. Sci. USA* **2004**, *101*, 12 814.
[16] W. Zheng, H. O. Jacobs, *Appl. Phys. Lett.* **2004**, *85*, 3635.
[17] W. Zheng, H. O. Jacobs, *Adv. Funct. Mater.* **2005**, *15*, 732.
[18] X. Xiong, Y. Hanein, J. Fang, Y. Wang, W. Wang, D. T. Schwartz, K. F. Bohringer, *J. Microelectromech. Syst.* **2003**, *12*, 117.
[19] C. R. Barry, C. J. Hoon, H. O. Jacob, presented at the *Int. Conf. on Foundations of NanoScience: Self-Assembled Architectures and Devices*, Snowbird, UT, USA, April **2004**.
[20] J. Chung, W. Zheng, H. O. Jacobs, presented at the *IEEE Int. Conf. on Micro Electro Mechanical Systems (MEMS)*, Miami Beach, FL, USA, January **2005**.
[21] S.-H. Liang, X. Xiong, K. F. Bohringer, presented at the *IEEE Int. Conf. on Micro Electro Mechanical Systems (MEMS)*, Maastricht, The Netherlands, January **2004**.
[22] J. Fang, K. F. Boringer, presented at the *IEEE Int. Conf. on Micro Electro Mechanical Systems (MEMS)*, Miami Beach, FL, USA, January **2005**.
[23] I. S. Choi, N. Bowden, G. M. Whitesides, *Angew. Chem. Int. Ed.* **1999**, *38*, 3078.
[24] I. S. Choi, N. Bowden, G. M. Whitesides, *J. Am. Chem. Soc.* **1999**, *121*, 1754.
[25] T. L. Breen, J. Tien, S. R. J. Oliver, T. Hadzic, G. M. Whitesides, *Science* **1999**, *284*, 948.

